Talanta 88 (2012) 175–180

Contents lists available at SciVerse ScienceDirect

Talanta

journal homepage: www.elsevier.com/locate/talanta

A microsecond microfluidic mixer for characterizing fast biochemical reactions

Ying Li[a], Dalu Zhang[b], Xiaojun Feng[a], Youzhi Xu[a,*], Bi-Feng Liu[a,*]

[a] Britton Chance Center for Biomedical Photonics at Wuhan National Laboratory for Optoelectronics – Hubei Bioinformatics & Molecular Imaging Key Laboratory, Department of Systems Biology, College of Life Science and Technology, Huazhong University of Science and Technology, Wuhan 430074, China
[b] China National Center for Biotechnology Development, Ministry of Science and Technology, Beijing 100039, China

ARTICLE INFO

Article history:
Received 19 August 2011
Received in revised form 18 October 2011
Accepted 22 October 2011
Available online 25 October 2011

Keywords:
Zigzag micromixer
Turbulent mixing
Chemiluminescence
Fast reaction

ABSTRACT

Analysis of fast biochemical reactions requires rapid mixing of solutions. Micromixers can achieve uniform mixing of solutions in a short time and have been recognized as an attractive tool to analyze fast reactions. However, it is still a challenge to design mixers with simple structure and short dead time. Here, a zigzag turbulent micromixer was developed with a rapid mixing time of 16 μs at sample consumption of 10 μL/s. Numerical simulations and confocal imaging validated this result. Application of the chemiluminescence (CL) reaction demonstrated the use of this mixer in analyzing the kinetic process of the CL reaction. In comparison to the turbulent micromixers reported previously, this zigzag mixer has advantages of short dead time, simple structure and low sample consumption. We anticipate the developed mixer to be a useful tool in studying biochemical kinetics or be integrated to Lab-on-a-chip device as a pretreatment functional unit.

1. Introduction

Rapid and efficient mixing is essential in chemical or biochemical analysis [1–4]. In order to characterize a rapid biochemical process, such as nanomaterial synthesis [5] or chemical kinetics [6–8], reagents must be rapidly mixed before significant progress of the reaction begins to occur. Recently, micromixer has been an attractive tool to resolve fast reactions as its rapid mixing and low sample consumption [9–16].

According to the principle of mixing, micromixers could be categorized into passive mixers and active mixers [17]. Active mixers have good performance in the mixing of solutions over a large volume with the help of external energy and complex structures [17–20], while passive mixers can achieve comparable mixing efficiency with simpler architectures. Besides, passive mixers are more compatible with biological samples than active mixers. Thus, they are preferred to researchers and many passive mixers have been designed and optimized recently [13,21–25].

For passive micromixers, rapid mixing is often achieved through hydrodynamic focusing (lamination) or turbulence [2,7,8]. As Reynolds number (Re) is small in microfluidic channel (Re < 2000), diffusion is the dominant transport mechanism between two fluid layers. According to the diffusion principle, the length scale for diffusion needs to be reduced to about 30 nm to achieve microsecond mixing for small molecules in aqueous solvents (the diffusion coefficient is $\sim 10^{-9}$ m^2 s^{-1}) [16]. To get a short mixing time, Brody et al. first designed a lamination mixer [26], which focused the center stream line to ~0.1 μm and achieved a mixing time of ~10 μs. Hertzog et al. [7] and Yao et al. [16] improved the mixing time of lamination mixer to 4 μs and 1 μs, respectively. However, these ultrarapid mixers were made of glass/silicon and had very small channel scale (<2 μm), making them difficult and costly to manufacture [7,14]. Besides, narrow microchannel may easily cause clogging issues [7].

As an alternative to lamination, mixers based on turbulence can also achieve rapid mixing. Turbulent mixers can stretch and fold the solution flow to generate narrow striations, which will exponentially increase the interfacial area between the solutions and cause rapid mixing in a short channel length. Turbulent mixing in microchannel can be realized through two ways. One is by modifying the interior channel, such as placing grooves and ribs in the flow path [27–29]. Stroock et al. [27] firstly designed a staggered herringbone mixer, which caused circulation flows leading to exponential increase of interface. Thus, fast mixing was achieved. However, the mixing time of this kind of mixer is usually at a millisecond time scale. The other way is by modifying the exterior channel, such as setting the channel as C-shape [30] or zigzag fashion [31]. Liu et al. [30] fabricated a serpentine microchannel with a "C-shaped" repeating unit. At Re = 70, the serpentine channel produced 16 times more product than the straight channel. Mengeaud et al. [31] simulated the mixing process of species in a zigzag microchannel using a finite element model. For Re = 267, the zigzag got best mixing efficiency. Egawa et al. [13] demonstrated a

* Corresponding authors. Tel.: +86 27 87792203; fax: +86 27 87792170.
E-mail addresses: yzxu@smail.hust.edu.cn (Y.Z. Xu), bfliu@mail.hust.edu.cn, bifeng_liu@yahoo.com (B.-F. Liu).

0039-9140/$ – see front matter © 2011 Elsevier B.V. All rights reserved.
doi:10.1016/j.talanta.2011.10.028

silicon T mixer followed by three repeats of an alcove, which was arranged in a zigzag fashion. At a sample flow rate of 20 μL/s, the mixer exhibited a mixing dead time of ~22 μs. However, it is still a challenge to design rapid mixers with simple structure and general manufacturing technique.

In this paper, we reported a new passive micromixer with a Y-shape junction, followed by a zigzag channel. Based on computational fluid dynamics simulation (CFD), an optimized zigzag mixer was designed and fabricated with standard soft-lithography technique. Confocal images indicated the zigzag channel generated efficient turbulent mixing. At a total volumetric flow rate of 10 μL/s (Re = 248.3), complete mixing could achieve in 16 μs. Further, application of CL reaction demonstrated this micromixer in the analysis of the kinetic process of the reaction. The exhibited zigzag micromixer has shown advantages such as rapid solution mixing, low sample consumption and ease of fabrication, making it an attractive tool for studying fast biochemistry reactions.

2. Experimental

2.1. CFD simulations

Numerical simulations were carried out to optimize the structure of the zigzag mixer by using the simulation software Fluent 6.1. The mixing efficiency was investigated using a 3D finite volume model. To establish this model, the following assumptions are proposed: (1) the viscosity and density of the fluid maintain constant as the concentration changes, the interfacial force between the fluids and the gravity are neglected; (2) the channel walls are supposed to be smooth and the medium is assumed to be continuous; (3) the boundary condition at the inlets is a uniform velocity profile with $u_y = u_z = 0\ \mathrm{m\,s^{-1}}$ and u_x defined according to the Reynolds number.

The solving procedure adopted is similar to the one described by Mendels et al. [32] where the fluids are treated as isothermal and incompressible Newtonian fluids following the Navier–Stokes equations.

$$\rho\frac{\partial u}{\partial \tau} + \rho u \cdot \nabla u = -\nabla P + \mu\nabla^2 u \quad (1)$$

$$\nabla \cdot u = 0 \quad (2)$$

where ρ is the density, τ the time, u the velocity vector, P the pressure and μ is the dynamic viscosity.

After Eqs. (1) and (2) are solved, the distribution of the species concentration can be obtained by solving the diffusion-convection equation (Eq. (3)).

$$\frac{\partial u}{\partial \tau} + Du \cdot \nabla c = D\nabla^2 c \quad (3)$$

where c is the concentration of the species and D is the molecular diffusion coefficient of the species. The Reynolds number is defined as

$$Re = \frac{\bar{u}D_h}{\nu} \quad (4)$$

where $\bar{u}$ is the average velocity in the channel, D_h is the hydraulic diameter defined as $D_h = wh/(w+h)$ for a rectangle channel (w and h are the width and height of the channel, respectively) and ν is the kinetic viscosity.

The fluid for the simulation is Newtonian with density (ρ) $10^3\ \mathrm{kg\,m^{-3}}$, viscosity ($\mu$) $10^{-3}\ \mathrm{Pa\,s}$ and diffusion coefficient (D) $4.9\times10^{-10}\ \mathrm{m^2\,s^{-1}}$ (fluorescein in water [33]). For the two inlets, one fluid is pure water, the other fluid is aqueous solution which contained the simulated solute. The solution concentration for the two inlets is set as 0 and 1. The criterion for convergence is for the increment in each variable to fall below 1×10^{-5}.

2.2. Chip fabrication

The micromixer was fabricated according to the rapid prototyping method previously reported [34]. In brief, SU-8 2100 (Gersteltec Sarl, Switzerland) mold was fabricated on a silicon wafer n type ⟨1 0 0⟩ using standard soft-lithography technique. The PDMS layer, made from a mixture of 10:1 (m/m) PDMS and curing agent (Sylgard 184, Dow Corning, USA), was fabricated by molding the SU-8 structure. Then the PDMS sheet was cut and peeled from the mold. Holes of the inlets and outlet were punched using a gauge needle. The PDMS was irreversibly bonded to a cover glass slide after treatment of oxygen plasma. Teflon tubes with steel needles were inserted into the punched holes and stuck with epoxy glue to get the final chip.

2.3. Materials

Chemicals such as fluorescein, sulforhodamine B, $Na_2B_4O_7{\cdot}10H_2O$, K_2HPO_4, KH_2PO_4, KI, H_2O_2 were purchased from Sinopharm Chemical Reagent (Shanghai, China). Horseradish peroxidase (HRP) was purchased from Beijing Biosynthesis Biotechnology Co., Ltd. (Beijing, China), 4-iodophenol was purchased from Alfa Aeser (USA) and Luminol was purchased from Wako (Japan).

Solutions of $1\times10^{-6}\ \mathrm{mol\,L^{-1}}$ fluorescein, $1\times10^{-6}\ \mathrm{mol\,L^{-1}}$ sulforhodamine B and $0.5\ \mathrm{mol\,L^{-1}}$ KI were dissolved in $0.1\ \mathrm{mol\,L^{-1}}$ borate buffer (pH 11.0); CL reagent (containing $2.5\ \mathrm{mmol\,L^{-1}}$ luminal, $4.5\ \mathrm{mmol\,L^{-1}}$ 4-iodophenol, $100\ \mathrm{mmol\,L^{-1}}$ H_2O_2) was dissolved in $0.01\ \mathrm{mol\,L^{-1}}$ phosphate buffer (pH 11.0); $5\times10^{-5}\ \mathrm{mol\,L^{-1}}$ HRP was dissolved in $0.01\ \mathrm{mol\,L^{-1}}$ phosphate buffer (pH 6.8), HRP with low concentration was diluted from the $5\times10^{-5}\ \mathrm{mol\,L^{-1}}$ stock solution before the experiment. All reagents were of analytical grade unless specified otherwise. All solutions were prepared with water purified by the Direct-Q system (Millipore, Bedford, MA, USA) and filtered with 0.45 μm sterilized syringe filters before used.

2.4. Optical imaging system and operation procedures

Experiments were performed on an inverted fluorescence microscope (IX71, Olympus, Japan) with a CCD camera (Evolve 512, photometrics, USA). The objective used was 10×/0.3. Mixing of sulforhodamine B and fluorescein was examined with filter cubes of U-MWG2 (510–550 nm band-pass filter, 570 nm diachronic mirror, 590 nm high-pass filter, Olympus, Japan) and U-MWIB2 (460–490 nm band-pass filter, 505 nm diachronic mirror, 510 nm high-pass filter, Olympus, Japan). Reaction of KI and fluorescein was examined with the filter cube of U-MWIB2. The luminescence of CL reaction was collected with a 420 nm high-pass emission filter.

Mixing of fluorescein and borate buffer was monitored with a confocal laser scanning microscopy (Olympus FV1000, Japan). A 488 nm Argon laser was used for exciting fluorescein. The objective used was 40×/1.35 oil and the spatial resolution of the image along the z-axis was set as 0.62 μm (as each pixel of the image was 0.62 μm × 0.62 μm at the x–y plane).

The solutions were injected into the two inlets of the zigzag mixer by a syringe pump (KDScientific, USA) with identical volumetric flow rate according to the desired Reynolds number. Acquired images were further analyzed using image pro plus 6.0, Matlab 7.0 and origin 7.5.

3. Results and discussion

3.1. CFD simulation

For the zigzag micromixer, two essential parameters that could affect the mixing efficiency were the turning angle of the zigzag

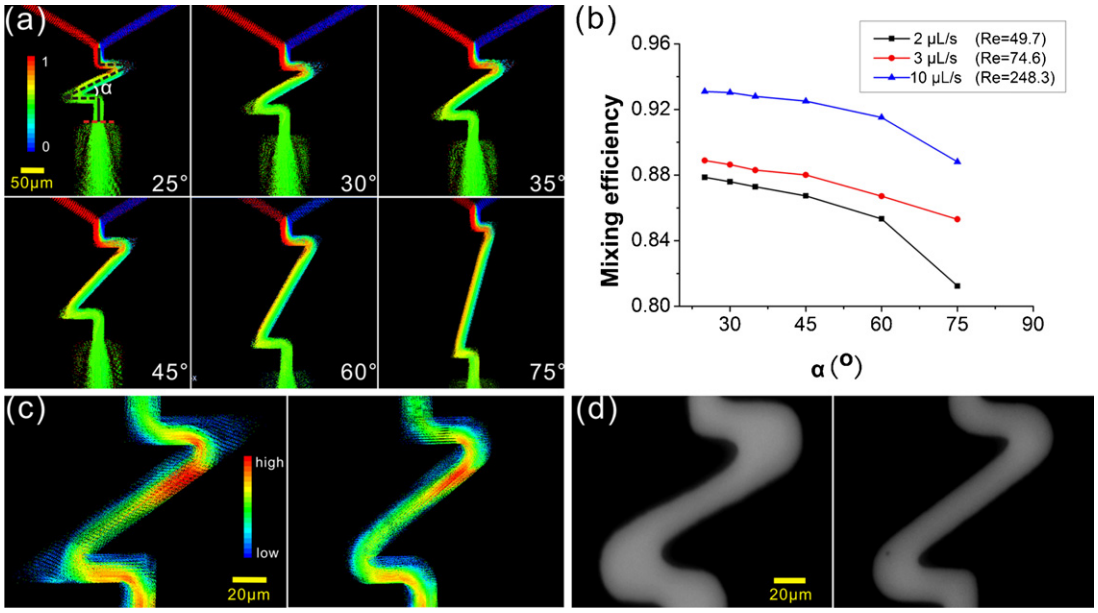

Fig. 1. Optimization of the zigzag mixer. (a) Simulation of the zigzag mixer with different turning angles (defined as α) at a flow rate of 10 μL/s. The position of the red dotted line was the end of the small outlet. The mixing length from the Y junction to the end of the small outlet was 320 μm (the length of the black dotted line and sum of the two black solid lines was 240 μm and 80 μm, respectively). (b) Mixing efficiency of various α at different flow rates. (c) Velocity vectors of the unchamfered (left) and chamfered (right) angle. (d) Chip fabricated with α of 30° (left) and 35° (right). The two corners of the fabricated chip with angle of 30° distorted for the limit of fabrication. (For interpretation of the references to color in this text, the reader is referred to the web version of this article.)

channel and the width of the small outlet. To design and optimize the geometry of the mixer, CFD simulation (Fluent 6.1) was employed.

The turning angle (defined as α) of the zigzag channel was investigated firstly. The line length of the zigzag channel was kept constant as 240 μm. Angles of 25°, 30°, 35°, 45°, 60° and 75° were examined (Fig. 1a). At total volumetric flow rates of 2 μL/s, 3 μL/s and 10 μL/s, the data showed that smaller α resulted in better mixing efficiency at the end of the small outlet (Fig. 1b). A possible reason could be that decreasing α resulted in increasing interfacial area, which reduced the diffusion distance between the two solutions and generated sufficient fluid mixing. In the series of simulated angles, the mixing efficiency was best when α was 25°. Due to the fabrication limit, the channel would distort if α was less than 30° (Fig. 1d). Thus, 35° was recognized as the optimum angle for α.

Although the introduction of the zigzag channel could disturb the flow efficiently, the vectors of velocity showed that dead volume existed at the two corners of the zigzag channel. To overcome this problem, the two acute angles were chamfered. The data showed that it could effectively decrease the dead volume (Fig. 1c).

Subsequently, the width of the small outlet channel was examined. Three widths of 12 μm, 20 μm and 30 μm were tested at the total volumetric flow rate of 10 μL/s. Results showed that the mixing efficiency at the end of the small outlet was better than 90% when the width was 12 μm and 20 μm, while the width of 30 μm achieved only 87%. In consideration of the chip fabrication (channels with small width are relatively difficult to fabricate and easily clogged), 20 μm was recognized as the optimum width for the small outlet.

In summary, we designed the zigzag mixer with geometry shown in Fig. 2a, the wide channel width 100 μm, the small channel width 20 μm, the turning angle α 35°, the total mixing length from the Y junction to the end of the small outlet 320 μm and the channel height 25 μm. The fabricated microfluidic chip was shown in Fig. 2b.

3.2. Experimental evaluation of the zigzag mixer

To examine the performance of the new zigzag mixer, sulforhodamine B and fluorescein were mixed in the fabricated chip. The two solutions were injected into the two inlets at a total volumetric flow rate of 10 μL/s. The color overlay image suggested complete mixing and fit well with the simulation result (Fig. 3b and c). To confirm the contribution of the zigzag channel to the mixing of the two solutions, a simple Y junction mixer was designed with identical mixing length and channel scale. Results showed that the mixing efficiency of the zigzag mixer was better than the mixer with a straight channel (Fig. 3a and b), which illustrated that existence of the zigzag channel significantly enhanced the mixing efficiency.

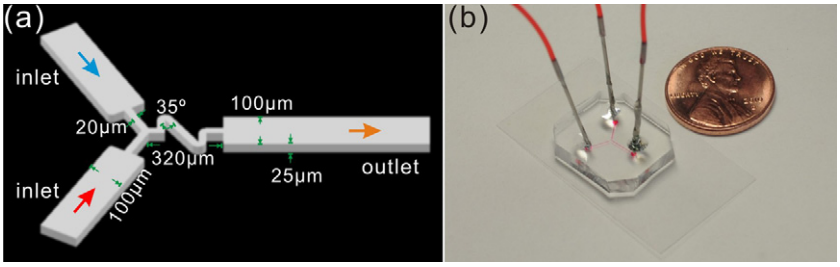

Fig. 2. (a) Schematic of the zigzag mixer. (b) The fabricated microfluidic chip (the coin used is U.S. one cent).

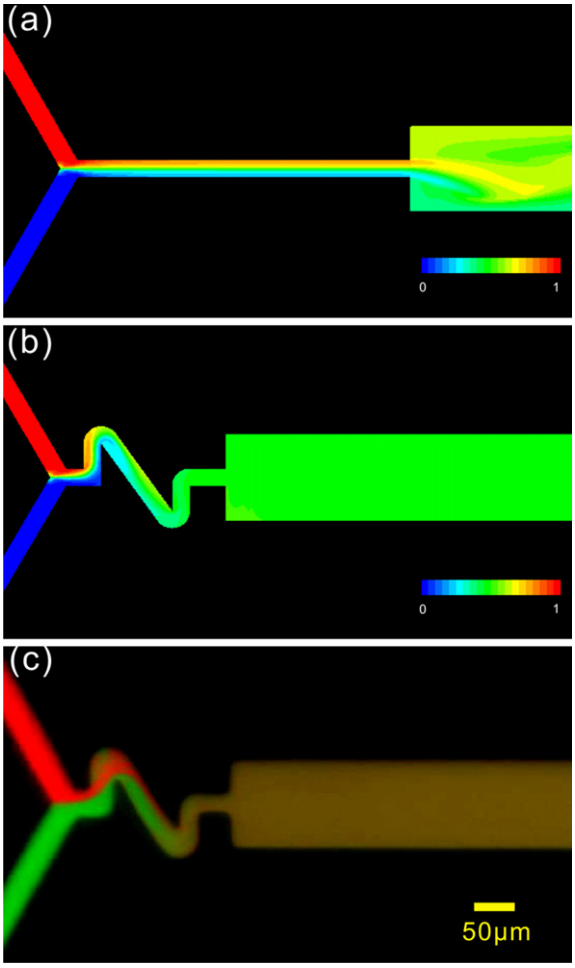

Fig. 3. Verification of the optimized zigzag mixer. (a) Simulation result of the mixer with a straight channel at a flow rate of 10 μL/s. (b) Simulation result of the zigzag mixer at a flow rate of 10 μL/s. (c) Experimental mixing of sulforhodamine B (red) and fluorescein (green) in the zigzag mixer at a flow rate of 10 μL/s. The color overlay image fit well with the simulation result shown in (b). (For interpretation of the references to color in this text, the reader is referred to the web version of this article.)

To further investigate the mixing process and the dead time of the zigzag mixer, we used confocal microscopy to examine the mixing of fluorescein and borate buffer. Sample flow rates of 0.67–10 μL/s were applied. The fluorescence distribution of the middle layer along the *z*-axis was shown as Fig. 4a. When the total volumetric flow rate was 0.67 μL/s (Re = 16.6), a clear fluid interface could be seen at the mixer outlet and nearly no mixing occurred between the two solutions. As the flow rate increased to 1.67 μL/s (Re = 41.4), interfacial turbulence emerged and mixing of the two solutions began to occur. After the flow rate further increased to 5 μL/s (Re = 124.2), the fluid interface showed obvious distortion and stretching. The two solutions interpenetrated when they flow through the two corners of the zigzag channel, which decreased the diffusion distance efficiently and accelerated the mixing evidently. Vortexes could be observed at the outlet, but solutions did not mix completely at this flow rate. When the flow rate rose to 10 μL/s (Re = 248.3), the interface stretched and folded further and complete mixing achieved at the end of the small outlet. Fig. 4b shows the reconstructed cross section and its surface plot at line A in Fig. 4a. Fig. 4c shows the reconstructed cross section and its surface plot at line B in Fig. 4a. All the reconstructed cross sections and their surface plots demonstrated similar fluorescence distribution between each slice along the *z*-axis. Especially, with the flow rate of 10 μL/s, the fluorescence at the *x*–*y* plane and *y*–*z* plane became both homogeneous from the end of the small outlet, which indicated complete mixing achieved at this flow rate. Thus, the end of the small outlet was determined to be the initial detection point.

To study the mixing efficiency quantitatively, the degree of mixing (C_m) was calculated according to the following equation [13,17]:

$$C_m = 1 - \frac{\sqrt{\sum (X_i - \bar{X})^2 / N}}{\bar{X}}$$

where X_i was the fluorescence intensity of each pixel in the cross section, N was the number of total pixels and $\bar{X}$ was the average fluorescence of all the pixels. Larger C_m indicated better mixing efficiency. Fig. 5a illustrated that when the flow rate increased to 10 μL/s, C_m at the initial detection point reached 90%, suggesting uniform fluorescence achieved here [13,33]. The fluorescence distribution across the channel at the initial detection point and 15 μm downstream to the initial detection point further indicated homogeneous fluorescence at this flow rate (Fig. 5b). In other words, the flow rate of 10 μL/s was sufficient to cause complete mixing at the initial detection point. To obtain the dead time of the zigzag mixer, a flow rate of 10 μL/s was used and C_m was calculated at various positions of the channel along the flow direction (Fig. 5c). According to the flow rate and the channel size (the flow rate was 10 μL/s and the volume of the mixing channel (V_m) was 1.6×10^{-13} m^3), we converted the Eulerian space coordinate to Lagrangian time coordinate [16]. The initial detection point achieved C_m of 90% and the mixing time was 16 μs (mixing time = V_m/flow rate [13]). Accordingly, the dead time of this zigzag mixer was determined to be 16 μs (Fig. 5d).

In comparison to the mixer previously reported [13], the proposed zigzag mixer achieved complete mixing based on a single zigzag unit, much simpler than the three repeated alcoves structure. In addition, induction of 6 μs mixing time (more than 25% improved) was realized with sample consumption of 10 μL/s, which was only a half of the flow rate used in the alcove-based mixer. Furthermore, this zigzag mixer had little dead volume in the mixing channel.

3.3. Application to chemical and biological reactions

Quench reaction of a fluorescent dye by iodide ions is a typical mixer characterization technique to determine the mixing efficiency [7,13]. To confirm the mixing efficiency of the new mixer, fluorescein and KI (a dynamic quencher of fluorescein) were applied at the flow rate of 10 μL/s (Re = 248.3). According to the result previously reported, 70% quenching of the fluorescence from fluorescein is expected upon complete mixing with 0.5 mol L^{-1} KI applied [13,35]. For the presented zigzag micromixer, homogeneous fluorescence was observed in the outlet channel. The fluorescence at the initial detection point (value = 14,869) was about 30% of the initial fluorescence (value = 49,752) at the inlet, which confirmed the two solutions achieved complete mixing in the mixer.

Chemiluminescence (CL) detection has advantages of wide linear range, no requirement for light source and rapid analysis time [36–38]. Luminol CL reaction catalyzed by HRP is usually coupled with immunoassay to quantitatively analyze antibody and antigen [39,40]. To examine the HRP concentration quantitatively, CL reagent and HRP with various concentrations were mixed in the zigzag mixer. The peak value of luminescence was extracted from the CL reaction curve. Based on eight different concentrations of HRP, calibration curve was established with linear dynamic range above three orders of magnitudes and linear correlation coefficient

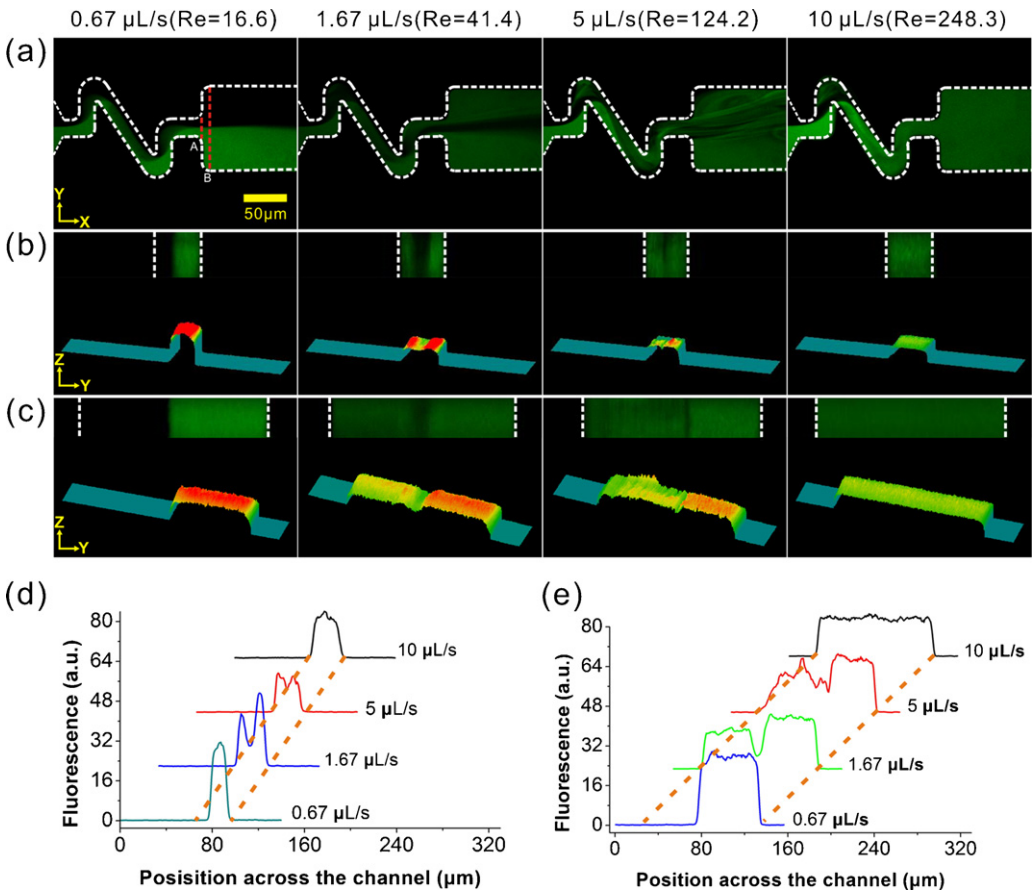

Fig. 4. Mixing of fluorescein and buffer at different flow rates (monitored with a confocal microscopy). (a) Fluorescence distribution of the middle layer along the *z* axis. (b) Reconstructed cross section and its surface plot at the end of the small outlet (line A in (a)). (c) Reconstructed cross section and its surface plot at the position of 15 μm downstream to the end of the small outlet (line B in (a)). (d) Fluorescence distribution across the channel at the end of the small outlet. (e) Fluorescence distribution across the channel at the position of 15 μm downstream to the end of the small outlet.

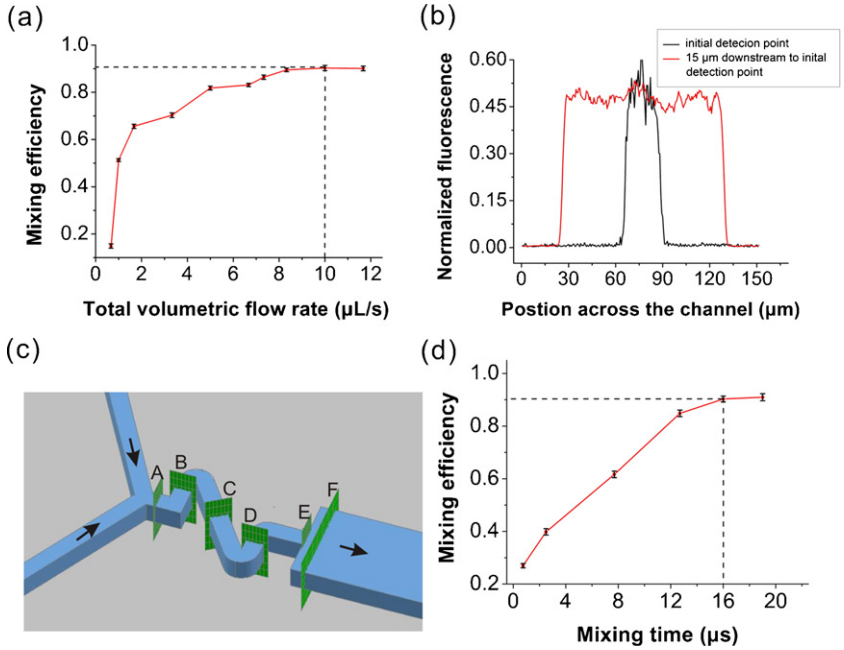

Fig. 5. Determining of the dead time of the zigzag mixer. (a) Mixing efficiency of various flow rates at the initial detection point. At the flow rate of 10 μL/s, the mixing efficiency achieved 90%, indicating complete mixing [13,33]. (b) Fluorescence distribution across the channel at the initial detection point (black) and 15 μm downstream to the initial detection point (red) at the flow rate of 10 μL/s. The normalized fluorescence value was ~ 0.5. (c) Positions along the channel for the calculation of the mixing time. (d) The dead time of the zigzag mixer. Based on the physical size and total volumetric flow rate, the dead time of the mixer was calculated to be 16 μs at a flow rate of 10 μL/s. (For interpretation of the references to color in this text, the reader is referred to the web version of this article.)

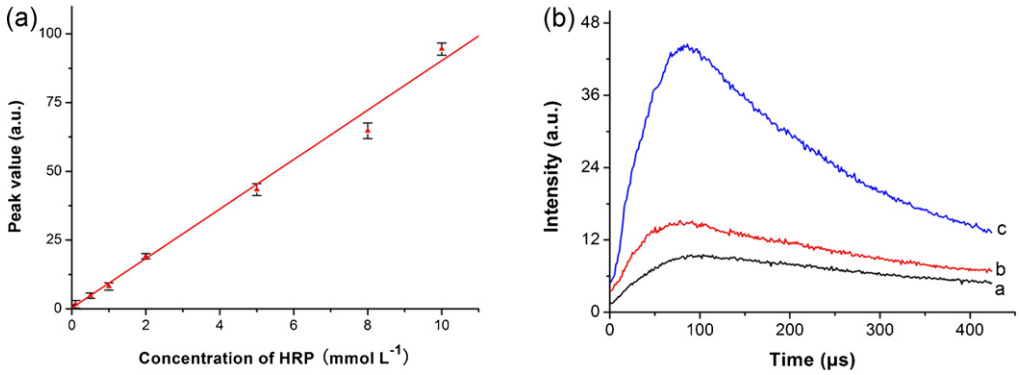

Fig. 6. Luminol-HRP CL reaction in the zigzag mixer. (a) Linear range of HRP concentration. The peak value of luminescence was extracted from the CL reaction curve; the linear range was from 0.01 mmol L^{-1} to 10 mmol L^{-1} with linear correlation coefficient $\gamma = 0.995$. (b) The kinetic process of luminol-HRP CL reaction. The zero point was the initial detection point and data of the three curves (a, 1×10^{-6} mol L^{-1} HRP; b, 2×10^{-6} mol L^{-1} HRP; c, 5×10^{-6} mol L^{-1} HRP) were extracted from the center line of the outlet channel.

$\gamma = 0.995$ (Fig. 6a). Thus, this mixer could further be served in quantitative analysis of CL reaction.

In Fig. 6b, three curves demonstrated the kinetic process of the CL reaction at different HRP concentrations. Since reagents of the CL reaction were mixed completely in a short time, the kinetic process of the subsequent reaction could be monitored continuously. The zero point of the three curves was the initial detection point and the peak value of the luminescence appeared in less than 100 μs. Thanks to its fast mixing capability, the zigzag mixer could initiate reactions rapidly, allowing the investigation of kinetics of fast reactions, such as the kinetics of protein folding at early stages.

4. Conclusion

Micromixers are essential components in the sample preparation stage of chemical analysis prior to chemical or biological reactions taking place. In this article, we proposed a new zigzag passive mixer and optimized the geometry with numerical simulation. The mixing efficiency was confirmed by the results of confocal microscopy. At a total volumetric flow rate of 10 μL/s (Re = 248.3), the zigzag micromixer achieved a dead time of 16 μs, which has been the shortest time among the PDMS micromixers with turbulent mixing. Further, we applied the zigzag mixer to examine the CL reaction, results showed that the micromixer had a wide linear range of HRP concentration and could track the kinetic process of the reaction. The zigzag micromixer presented here has simple structure and rapid mixing time. Moreover, the device is made of PDMS, making it simple to fabricate and replicate with a high fidelity. We anticipate this zigzag mixer will be a useful tool to study the folding kinetics of macromolecules and analyze other fast biochemistry processes. In addition, potential integration of the developed micromixer into more sophisticated micrototal analysis system can also be expected.

Acknowledgements

The authors gratefully acknowledge the financial supports from National Basic Research Program of China (2007CB914203, 2007CB714507) and National Natural Science Foundation of China (30970692, 21075045).

References

[1] J. Kubelka, J. Hofrichter, W.A. Eaton, Curr. Opin. Struct. Biol. 14 (2004) 76–88.
[2] H. Roder, K. Maki, H. Cheng, Chem. Rev. 106 (2006) 1836–1861.
[3] A. Hoffmann, A. Kane, D. Nettels, D.E. Hertzog, P. Baumgärtel, J. Lengefeld, G. Reichardt, D.A. Horsley, R. Seckler, O. Bakajin, B. Schuler, Proc. Natl. Acad. Sci. U.S.A. 104 (2007) 105–110.
[4] E.A. Alemán, R. Lamichhane, D. Rueda, Curr. Opin. Chem. Biol. 12 (2008) 647–654.
[5] J. deMello, A. deMello, Lab Chip 4 (2004) 11N–15N.
[6] M.C. Ramachandra Shastry, J.M. Sauder, H. Roder, Acc. Chem. Res. 31 (1998) 717–725.
[7] D.E. Hertzog, B. Ivorra, B. Mohammadi, O. Bakajin, J.G. Santiago, Anal. Chem. 78 (2006) 4299–4306.
[8] S. Matsumoto, A. Yane, S. Nakashima, M. Hashida, M. Fujita, Y. Goto, S. Takahashi, J. Am. Chem. Soc. 129 (2007) 3840–3841.
[9] P. Regenfuss, R.M. Clegg, M.J. Fulwyler, F.J. Barrantes, T.M. Jovin, Rev. Sci. Instrum. 56 (1985) 283–290.
[10] M.C.R. Shastry, S.D. Luck, H. Roder, Biophys. J. 74 (1998) 2714–2721.
[11] O. Bilsel, C. Kayatekin, L.A. Wallace, C.R. Matthews, Rev. Sci. Instrum. 76 (2005) 0143021–0143027.
[12] H.Y. Park, X. Qiu, E. Rhoades, J. Korlach, L.W. Kwok, W.R. Zipfel, W.W. Webb, L. Pollack, Anal. Chem. 78 (2006) 4465–4473.
[13] T. Egawa, J.L. Durand, E.Y. Hayden, D.L. Rousseau, S.-R. Yeh, Anal. Chem. 81 (2009) 1622–1627.
[14] Y. Gambin, C. Simonnet, V. VanDelinder, A. Deniz, A. Groisman, Lab Chip 10 (2010) 598–609.
[15] X. Mao, B. Juluri, M. Lapsley, Z. Stratton, T. Huang, Microfluid. Nanofluid. 8 (2010) 139–144.
[16] S. Yao, O. Bakajin, Anal. Chem. 79 (2007) 5753–5759.
[17] N.T. Nguyen, Z. Wu, J. Micromech. Microeng. 15 (2005) R1–R16.
[18] L.H. Lu, K.S. Ryu, C. Liu, J. Microelectromech. Syst. 11 (2002) 462–469.
[19] H. Mao, T. Yang, P.S. Cremer, J. Am. Chem. Soc. 124 (2002) 4432–4435.
[20] N. Sasaki, T. Kitamori, H.B. Kim, Lab Chip 6 (2006) 550–554.
[21] R. Choudhary, T. Bhakat, R.K. Singh, A. Ghubade, S. Mandal, A. Ghosh, A. Rammohan, A. Sharma, S. Bhattacharya, Microfluid. Nanofluid. 10 (2010) 271–286.
[22] T. Kang, M. Singh, P. Anderson, H. Meijer, Microfluid. Nanofluid. 7 (2009) 783–794.
[23] Z.H. Lu, J. McMahon, H. Mohamed, D. Barnard, T.R. Shaikh, C.A. Mannella, T. Wagenknecht, T.M. Lu, Sens. Actuators B 144 (2010) 301–309.
[24] T. Tofteberg, M. Skolimowski, E. Andreassen, O. Geschke, Microfluid. Nanofluid. 8 (2010) 209–215.
[25] H.M. Xia, Z.P. Wang, Y.X. Koh, K.T. May, Lab Chip 10 (2010) 1712–1716.
[26] J.P. Brody, P. Yager, R.E. Goldstein, R.H. Austin, Biophys. J. 71 (1996) 3430–3441.
[27] A.D. Stroock, S.K.W. Dertinger, A. Ajdari, I. Mezić, H.A. Stone, G.M. Whitesides, Science 295 (2002) 647–651.
[28] Y. Lin, G.J. Gerfen, D.L. Rousseau, S.-R. Yeh, Anal. Chem. 75 (2003) 5381–5386.
[29] J.P.B. Howell, D.R. Mott, S. Fertig, C.R. Kaplan, J.P. Golden, E.S. Oran, F.S. Ligler, Lab Chip 5 (2005) 524–530.
[30] R.H.S. Liu, M.A. Stremler, K.V. Sharp, M.G. Olsen, J.G. Santiago, R.J. Adrian, H. Aref, D.J. Beebe, J. Microelectromech. Syst. 9 (2000) 190–197.
[31] V. Mengeaud, J. Josserand, H.H. Girault, Anal. Chem. 74 (2002) 4279–4286.
[32] D.A. Mendels, E. Graham, S. Magennis, A. Jones, F. Mendels, Microfluid. Nanofluid. 5 (2008) 603–617.
[33] T. Shih, C. Chung, Microfluid. Nanofluid. 5 (2008) 175–183.
[34] D.C. Duffy, J.C. McDonald, O.J.A. Schueller, G.M. Whitesides, Anal. Chem. 70 (1998) 4974–4984.
[35] J.R. Albani, Biochim. Biophys. Acta 1425 (1998) 405–410.
[36] P. Fletcher, K.N. Andrew, A.C. Calokerinos, S. Forbes, P.J. Worsfold, Luminescence 16 (2001) 1–23.
[37] B.F. Liu, M. Ozaki, Y. Utsumi, T. Hattori, S. Terabe, Anal. Chem. 75 (2002) 36–41.
[38] J.L. Adcock, P.S. Francis, N.W. Barnett, Anal. Chim. Acta 601 (2007) 36–67.
[39] K. Hatakeyama, T. Tanaka, M. Sawaguchi, A. Iwadate, Y. Mizutani, K. Sasaki, N. Tateishi, T. Matsunaga, Lab Chip 9 (2009) 1052–1058.
[40] Z. Wang, S.Y. Chin, C.D. Chin, J. Sarik, M. Harper, J. Justman, S.K. Sia, Anal. Chem. 82 (2009) 36–40.